

Electronic Supplementary Information

Insights into Mechanism and Selectivity in Rh(I)-catalyzed

Cycloisomerization Reaction of Benzylallene-Alkynes involving C–H Bond

Activation

Ying Ren,*^a Tilong Yang,^b and Zhenyang Lin*^{a,b}

^a Key Laboratory of Magnetic Molecules & Magnetic Information Materials Ministry of Education, The School of Chemistry and Material Science, Shanxi Normal University, Taiyuan, China

^b Department of Chemistry, The Hong Kong University of Science and Technology, Clear Water Bay, Kowloon, Hong Kong, China

Contents:

Fig. S1 Gibbs energy profiles calculated for the terminal alkyne C–H oxidative addition step. The solvation-corrected relative Gibbs energies and electronic energies (in parentheses) are given in kcal mol ⁻¹	S2
Fig. S2 Gibbs energy profile calculated for the oxidative coupling (A1' _H → B1' _H). The solvation-corrected relative Gibbs energies and electronic energies (in parentheses) are given in kcal mol ⁻¹	S3
Fig. S3 Gibbs energy profiles calculated for C → G (bond rotation) to give Me-product 4_{Me} , according to Scheme 2. Relative Gibbs energies and electronic energies (in parentheses) are given in kcal mol ⁻¹	S4
Fig. S4 Gibbs energy profiles calculated for (a) C → D (insertion), (b) D → F (β -hydride elimination) followed by F → A (reductive elimination) to give Me-product 3_{tBu} , and (c) C → G (bond rotation) followed by G → A (reductive elimination) to give Me-product 4_{tBu} , according to Scheme 2. Relative Gibbs energies and electronic energies (in parentheses) are given in kcal mol ⁻¹	S5
Fig. S5 Optimized structures for some key transition states for reactions of the benzylallene-alkyne substrates having Y = SO ₂ Ph (EDG), R ¹ = H; Y = SO ₂ Ph (EDG), R ¹ = Me; Y = Me (EWG), R ¹ = Me; and Y = tBu (EWG), R ¹ = Me..	S6
Table S1 Zero-point energies (ZPE), Total electronic energies (E), Gibbs energies (G), Total electronic energies (E _{solvation}), and Gibbs energies (G _{solvation}) of solvation (in a.u.) for all species involved in the catalytic cycles.	S7
Table S2 Results of BMK single-point energy calculations for all the species shown in Fig. 1 on the basis of the M06-optimized structures.....	S11

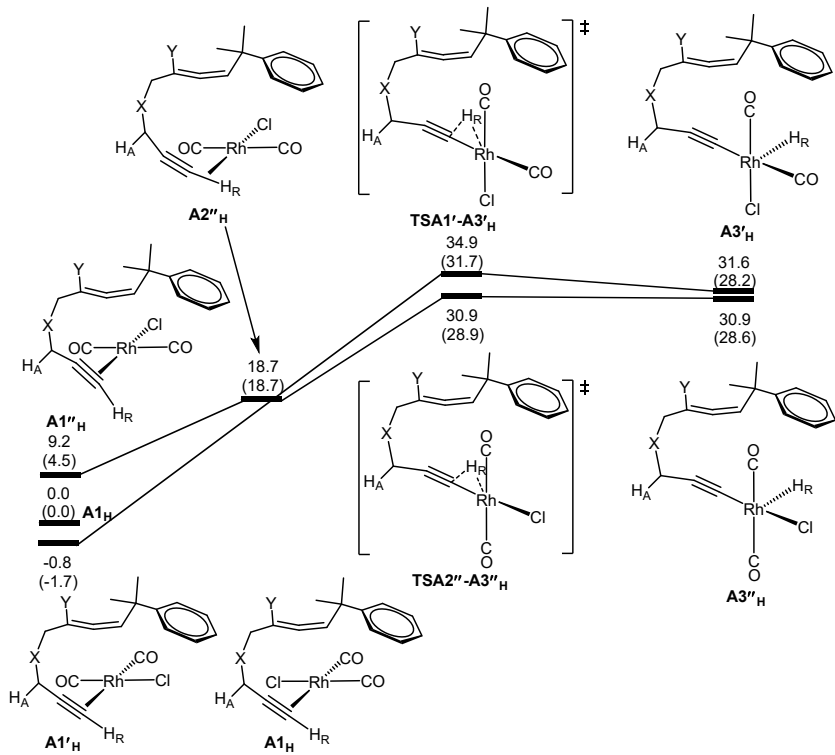


Fig. S1 Gibbs energy profiles calculated for the terminal alkyne C–H oxidative addition step. The solvation-corrected relative Gibbs energies and electronic energies (in parentheses) are given in kcal mol⁻¹.

Oxidative addition occurs between the acetylenic C–H bond with Rh^I in the substrate-coordinated from $\mathbf{A1'}_\text{H}$ and $\mathbf{A1''}_\text{H}$. The reaction begins with terminal alkyne of substrate $\mathbf{1}_\text{H}$ binding the Rh(CO)₂Cl giving three isomers ($\mathbf{A1'}_\text{H}$, $\mathbf{A1''}_\text{H}$, and $\mathbf{A1'''}_\text{H}$) as illustrated in Fig. S1. The main difference among the three isomers is the different ligands coordinating to the Rh center. $\mathbf{A1''}_\text{H}$ is most unstable mainly due to *trans* influence. $\mathbf{A1'}_\text{H}$ is calculated to be about 0.8 kcal mol⁻¹ more stable than $\mathbf{A1''}_\text{H}$. The oxidative addition step goes via the transition states, $\mathbf{TSA1'-A3'_H}$ and $\mathbf{TSA2''-A3''_H}$ leading to the transition metal hydride intermediates $\mathbf{A3'_H}$ and $\mathbf{A3''_H}$, respectively. It is can be seen that the step $\mathbf{A1''}_\text{H} \rightarrow \mathbf{A3''_H}$ is more favorable than that of $\mathbf{A1'}_\text{H} \rightarrow \mathbf{A3'_H}$. The Gibbs energy profiles in Fig. S1 illustrate that the proton migration steps ($\mathbf{A1'}_\text{H} \rightarrow \mathbf{A3'_H}$ and $\mathbf{A1''}_\text{H} \rightarrow \mathbf{A3''_H}$) are endergonic by 31.6 and 30.9 kcal mol⁻¹ and need to overcome the higher Gibbs energy barriers of 34.9 and 30.9 kcal mol⁻¹.

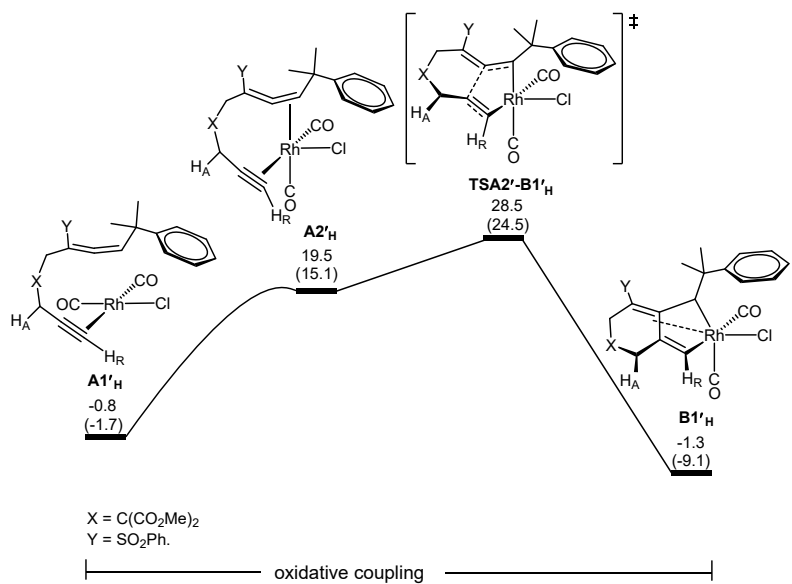


Fig. S2 Gibbs energy profile calculated for the oxidative coupling ($A1'H \rightarrow B1'H$). The solvation-corrected relative Gibbs energies and electronic energies (in parentheses) are given in kcal mol⁻¹.

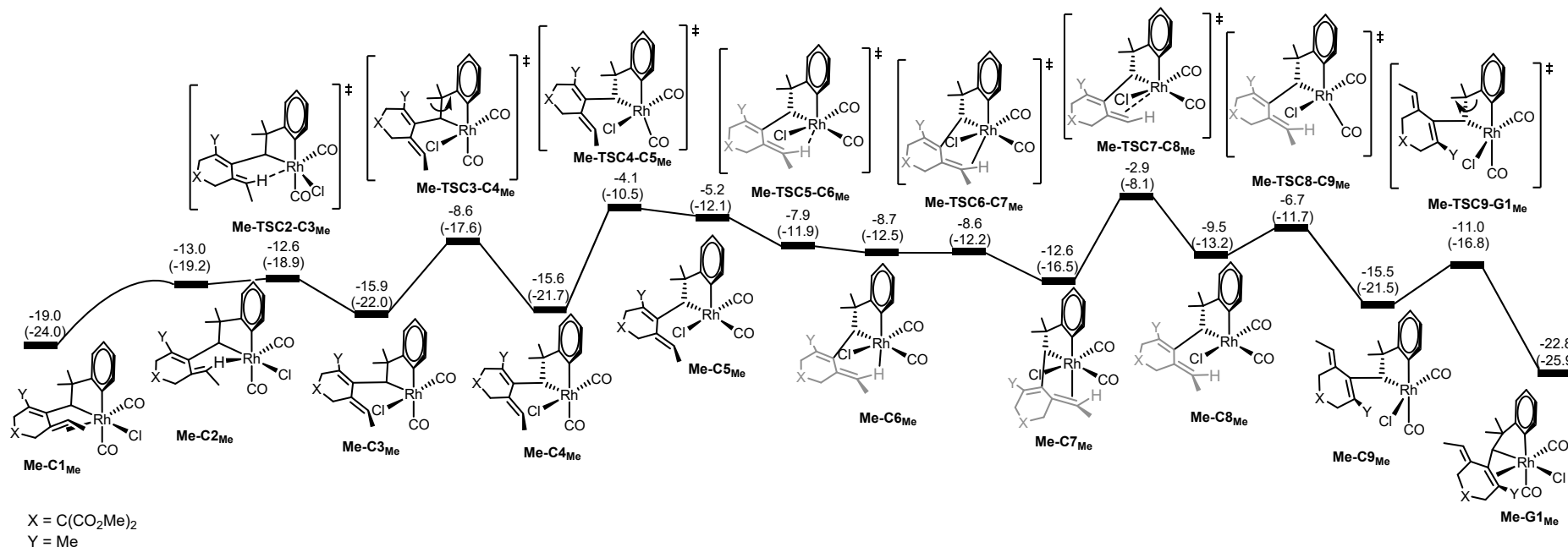


Fig. S3 Gibbs energy profiles calculated for **C** → **G** (bond rotation) to give **Me-product 4_{Me}**. Relative Gibbs energies and electronic energies (in parentheses) are given in kcal mol⁻¹.

Fig. S3 shows the energy profile calculated for the bond rotation step from **Me-C1_{Me}** to **Me-G1_{Me}**. Based on the structure of intermediate **Me-C1_{Me}**, ligand exchange takes place to produce the **Me-C2_{Me}**. Then dissociation of the C–H_R moiety from the metal center affords the intermediate **Me-C3_{Me}**. In order to facilitate the bond rotation, conformational change of the five membered ring in **Me-C3_{Me}** occurs to give the intermediate **Me-C4_{Me}**. **Me-C4_{Me}** further undergoes structural rearrangement to form the intermediate **Me-C5_{Me}**. With the C_{sp²}–C_{sp³}(Rh) bond rotation, the Rh center and the active site on the substrate skeleton of the intermediate **Me-C5_{Me}** undergo a stepwise ligand exchange to generate the intermediate **Me-C8_{Me}**. From the intermediate **Me-C8_{Me}**, structural rearrangement gives the intermediate **Me-C9_{Me}**. Subsequently, conformational change of the five-membered ring in **Me-C9_{Me}** affords the intermediate **Me-G1_{Me}**. As shown in Fig. S3, the bond rotation steps from **Me-C1_{Me}** to **Me-G1_{Me}** involves a series of conformation changes with accessible barriers.

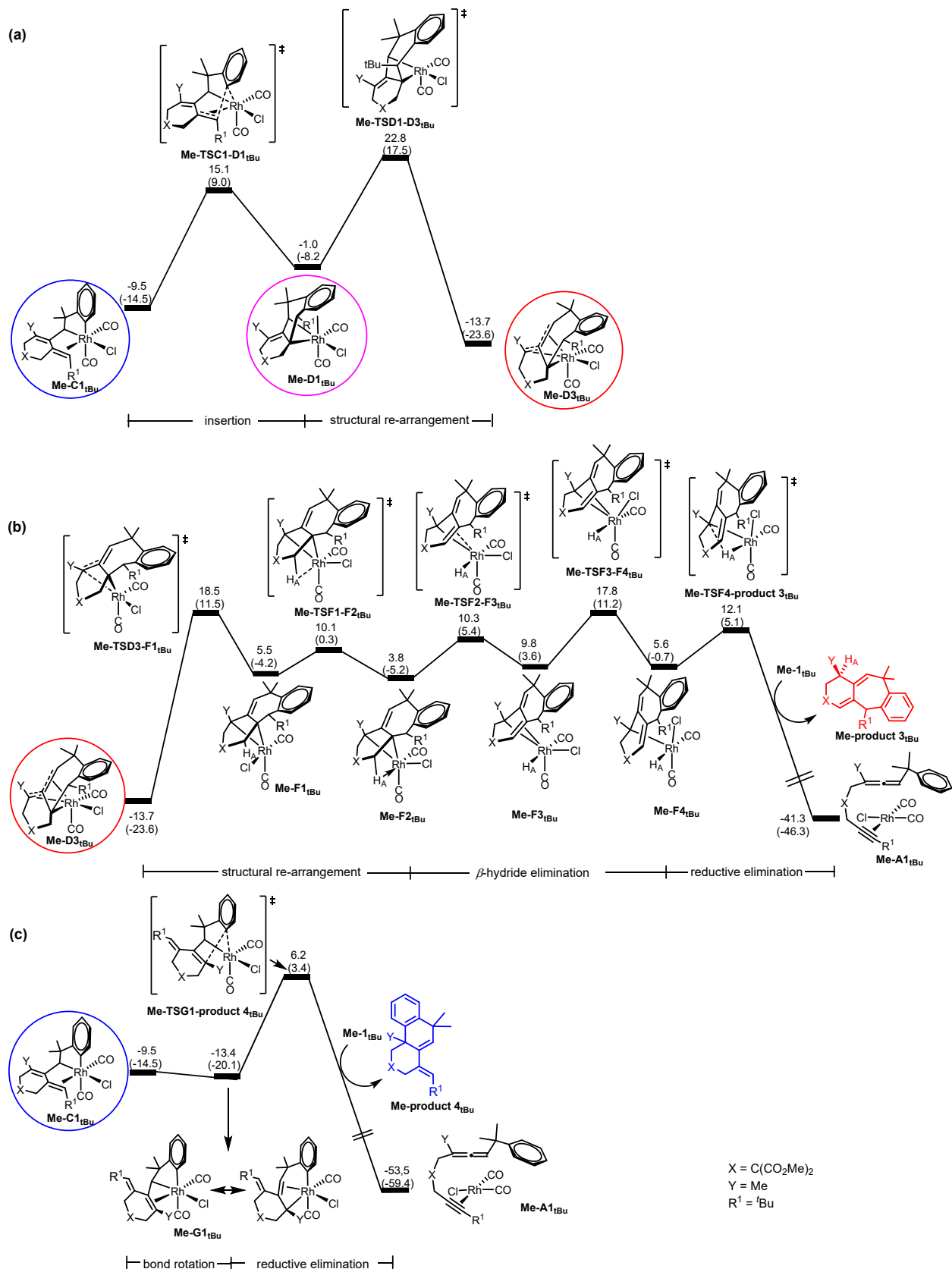


Fig. S4 Gibbs energy profiles calculated for (a) **C** → **D** (insertion), (b) **D** → **F** (β -hydride elimination) followed by **F** → **A** (reductive elimination) to give **Me-product 3_{tBu}**, and (c) **C** → **G** (bond rotation) followed by **G** → **A** (reductive elimination) to give **Me-product 4_{tBu}**, according to Scheme 2. Relative Gibbs energies and electronic energies (in parentheses) are given in kcal mol⁻¹.

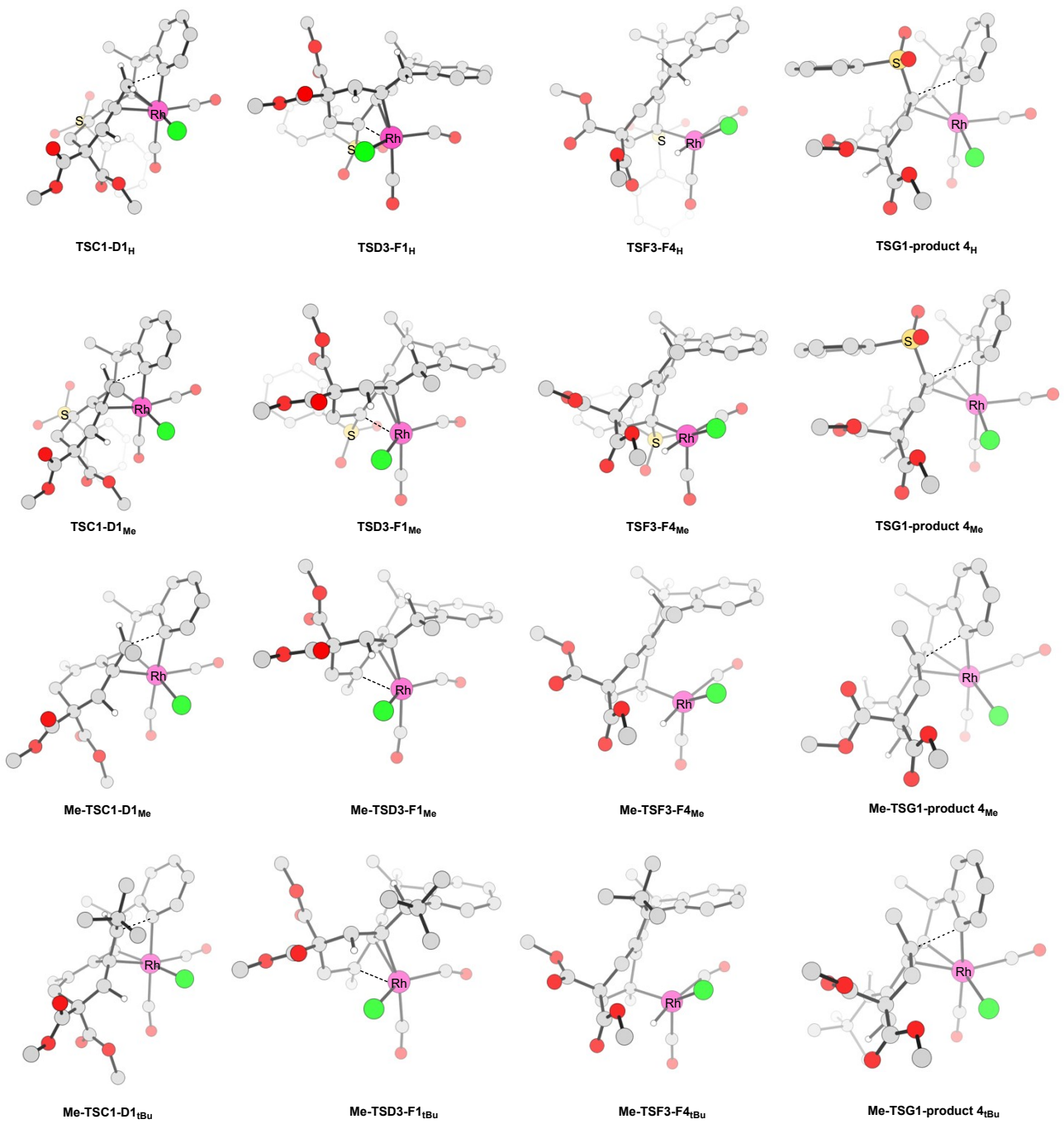


Fig. S5 Optimized structures for some key transition states for reactions of the benzylallene-alkyne substrates having Y = SO₂Ph (EDG), R¹ = H; Y = SO₂Ph (EDG), R¹ = Me; Y = Me (EWG), R¹ = Me; and Y = tBu (EWG), R¹ = Me.

Table S1 Zero-point energies (*ZPE*), Total electronic energies (*E*), Gibbs energies (*G*), Total electronic energies (*E_{solvation}*), and Gibbs energies (*G_{solvation}*) of solvation (in a.u.) for all species involved in the catalytic cycles.

Structure	<i>ZPE</i>	<i>E</i>	<i>G</i>	<i>E_{solvation}</i>	<i>G_{solvation}</i>
1_H	0.495279	-1506.0292183	-1505.629223	-1506.4395045	-1506.039509
A1'_H	0.513752	-1857.1355301	-1856.736745	-1857.6080227	-1857.209238
A1''_H	0.515022	-1857.1246548	-1856.719827	-1857.5981313	-1857.193304
A2'_H	0.514247	-1857.1041141	-1856.699623	-1857.5813053	-1857.176814
A2''_H	0.512314	-1857.1006799	-1856.703176	-1857.57558	-1857.178076
TSA1'-A3'_H	0.511353	-1857.0788223	-1856.67631	-1857.554813	-1857.1523
TSA2''-A3''_H	0.511190	-1857.0828893	-1856.682342	-1857.559274	-1857.158727
A3'_H	0.512611	-1857.0838586	-1856.68096	-1857.560484	-1857.157585
A3''_H	0.512316	-1857.0828146	-1856.681828	-1857.559724	-1857.158738
TSA2'-B1'_H	0.514095	-1857.0968186	-1856.692946	-1857.566336	-1857.162463
B1'_H	0.516529	-1857.1519068	-1856.741956	-1857.619917	-1857.209966
A1_H	0.512997	-1857.126939	-1856.729475	-1857.605376	-1857.207912
A2_H	0.515504	-1857.1182257	-1856.711713	-1857.589624	-1857.183111
TSA2-B1_H	0.512837	-1857.1012274	-1856.699837	-1857.569708	-1857.168318
B1_H	0.517956	-1857.1484404	-1856.740796	-1857.618453	-1857.210809
TSB1-B2_H	0.517930	-1857.1483429	-1856.738056	-1857.618228	-1857.207941
B2_H	0.517663	-1857.1717797	-1856.761198	-1857.640051	-1857.229469
TSB2-B3_H	0.517438	-1857.1439232	-1856.733973	-1857.614377	-1857.204427
B3_H	0.518705	-1857.168334	-1856.759768	-1857.637651	-1857.229085
TSB3-B4_H	0.517284	-1857.1397583	-1856.72894	-1857.611406	-1857.200588
B4_H	0.518854	-1857.1766559	-1856.764173	-1857.645513	-1857.23303
TSB4-C1_H	0.513540	-1857.1476413	-1856.737635	-1857.615697	-1857.20569
C1_H	0.519052	-1857.1742701	-1856.758809	-1857.640461	-1857.225
TSC1-D1_H	0.518153	-1857.1566409	-1856.741082	-1857.622445	-1857.206886
D1_H	0.520415	-1857.201682	-1856.785774	-1857.666577	-1857.250669
TSD1-D2_H	0.518859	-1857.1753786	-1856.762566	-1857.644623	-1857.23181
D2_H	0.521106	-1857.1925504	-1856.776172	-1857.660882	-1857.244504
TSD2-D3_H	0.518491	-1857.1761417	-1856.765353	-1857.644737	-1857.233948
D3_H	0.520631	-1857.2200328	-1856.803875	-1857.686182	-1857.270024
TSD1-E1_H	0.520012	-1857.173459	-1856.757508	-1857.639757	-1857.223806
E1_H	0.520365	-1857.1898738	-1856.773007	-1857.658511	-1857.241644
TSE1-E2_H	0.516234	-1857.1724966	-1856.759794	-1857.64062	-1857.227917
E2_H	0.517236	-1857.1739886	-1856.760428	-1857.642415	-1857.228855
TSE2-E3_H	0.517439	-1857.1710471	-1856.757543	-1857.637128	-1857.223624
E3_H	0.519177	-1857.1824076	-1856.766587	-1857.648284	-1857.232464
TSE3-product2_H	0.517735	-1857.173403	-1856.7591	-1857.640245	-1857.225942

product2	0.502111	-1506.1550629	-1505.743899	-1506.551836	-1506.140672
TSD3-F1_H	0.518413	-1857.1624025	-1856.747638	-1857.629111	-1857.214346
F1_H	0.520262	-1857.1819971	-1856.765556	-1857.649489	-1857.233048
TSF1-F2_H	0.519853	-1857.1817605	-1856.763904	-1857.648917	-1857.23106
F2_H	0.518761	-1857.1916553	-1856.77872	-1857.662251	-1857.249316
TSF2-F3_H	0.516086	-1857.173307	-1856.760591	-1857.643214	-1857.230498
F3_H	0.517272	-1857.1745033	-1856.759946	-1857.644579	-1857.230022
TSF3-F4_H	0.514700	-1857.1546523	-1856.748038	-1857.623378	-1857.216764
F4_H	0.516593	-1857.1731571	-1856.763732	-1857.64285	-1857.233425
TSF4-product 3_H	0.514729	-1857.1593781	-1856.751351	-1857.627847	-1857.219819
product3_H	0.501234	-1506.1412085	-1505.733827	-1506.544105	-1506.136723
G1_H	0.517128	-1857.1612553	-1856.750648	-1857.627768	-1857.217161
TSG1-product 4_H	0.516322	-1857.1365389	-1856.722667	-1857.600467	-1857.186596
product 4_H	0.501405	-1506.1417999	-1505.728488	-1506.53893	-1506.125618
1_{Me}	0.524446	-1545.3217583	-1544.894517	-1545.740332	-1545.313091
A1_{Me}	0.542992	-1896.4241495	-1895.997983	-1896.90976	-1896.483594
C1_{Me}	0.547233	-1896.4660641	-1896.02447	-1896.940614	-1896.499019
TSC1-D1_{Me}	0.547055	-1896.4473308	-1896.002935	-1896.920417	-1896.476021
D1_{Me}	0.550190	-1896.4776754	-1896.031303	-1896.950778	-1896.504405
TSD1-D2_{Me}	0.548607	-1896.4476361	-1896.004302	-1896.92392	-1896.480586
D2_{Me}	0.550122	-1896.4607746	-1896.017058	-1896.936486	-1896.492769
TSD2-D3_{Me}	0.547937	-1896.4470208	-1896.006359	-1896.922854	-1896.482192
D3_{Me}	0.549247	-1896.4925648	-1896.050485	-1896.967081	-1896.525001
TSD3-F1_{Me}	0.546211	-1896.4418785	-1896.001822	-1896.916435	-1896.476379
F1_{Me}	0.548157	-1896.464714	-1896.022596	-1896.939694	-1896.497576
TSF1-F2_{Me}	0.547394	-1896.4598163	-1896.017071	-1896.9369	-1896.494155
F2_{Me}	0.546720	-1896.4688178	-1896.028328	-1896.947259	-1896.506769
TSF2-F3_{Me}	0.544588	-1896.449319	-1896.010436	-1896.927532	-1896.488649
F3_{Me}	0.545211	-1896.4503333	-1896.012238	-1896.928312	-1896.490216
TSF3-F4_{Me}	0.545529	-1896.4368261	-1895.997401	-1896.912705	-1896.473279
F4_{Me}	0.544954	-1896.4525483	-1896.01516	-1896.930271	-1896.492883
TSF4-product 3_{Me}	0.542945	-1896.4386092	-1896.003734	-1896.915355	-1896.48048
product 3_{Me}	0.528928	-1545.4214201	-1544.987043	-1545.832726	-1545.398348
G1_{Me}	0.545935	-1896.4513063	-1896.012246	-1896.925839	-1896.486779
TSG1-product 4_{Me}	0.544644	-1896.4240394	-1895.984794	-1896.896284	-1896.457039
product 4_{Me}	0.528551	-1545.4312544	-1544.992357	-1545.836479	-1545.397582
Me-1_{Me}	0.461345	-1193.2981254	-1192.917074	-1193.619266	-1193.238214
Me-A1_{Me}	0.479807	-1544.3999462	-1544.023178	-1544.788455	-1544.411687
Me-C1_{Me}	0.481574	-1544.4466635	-1544.061823	-1544.826764	-1544.441923
Me-TSC1-D1_{Me}	0.480671	-1544.4219385	-1544.036448	-1544.799816	-1544.414326

Me-D1_{Me}	0.484391	-1544.449346	-1544.060566	-1544.826645	-1544.437865
Me-TSD1-D2_{Me}	0.484106	-1544.4267771	-1544.035487	-1544.805676	-1544.414386
Me-D2_{Me}	0.484833	-1544.4460984	-1544.056483	-1544.827806	-1544.438191
Me-TSD2-D3_{Me}	0.484090	-1544.428946	-1544.039348	-1544.810013	-1544.420415
Me-D3_{Me}	0.485919	-1544.473342	-1544.0822	-1544.851678	-1544.460536
Me-TSD3-F1_{Me}	0.483789	-1544.4283153	-1544.037857	-1544.807755	-1544.417296
Me-F1_{Me}	0.484390	-1544.4471038	-1544.058689	-1544.826833	-1544.438418
Me-TSF1-F2_{Me}	0.482899	-1544.4404172	-1544.051233	-1544.822917	-1544.433732
Me-F2_{Me}	0.482831	-1544.4442285	-1544.05796	-1544.827209	-1544.44094
Me-TSF2-F3_{Me}	0.479733	-1544.4253612	-1544.040948	-1544.808472	-1544.424059
Me-F3_{Me}	0.480868	-1544.4265134	-1544.043831	-1544.809515	-1544.426832
Me-TSF3-F4_{Me}	0.481518	-1544.413952	-1544.026881	-1544.795457	-1544.408386
Me-F4_{Me}	0.481167	-1544.4297629	-1544.04272	-1544.811579	-1544.424536
Me-TSF4-product 3_{Me}	0.479717	-1544.4202442	-1544.035583	-1544.80251	-1544.417849
Me-product 3_{Me}	0.466779	-1193.3940097	-1193.008202	-1193.705767	-1193.31996
Me-G1_{Me}	0.482944	-1544.4491199	-1544.067388	-1544.829685	-1544.447953
Me-TSG1-product 4_{Me}	0.480063	-1544.4207341	-1544.038282	-1544.799327	-1544.416875
Me-product 4_{Me}	0.465973	-1193.4108302	-1193.024144	-1193.720872	-1193.334186
Me-1_{tBu}	0.545365	-1311.1504772	-1310.695275	-1311.498796	-1311.043594
Me-A1_{tBu}	0.564212	-1662.2630888	-1661.808024	-1662.67551	-1662.220445
Me-C1_{tBu}	0.566932	-1662.2930019	-1661.829939	-1662.698663	-1662.2356
Me-TSC1-D1_{tBu}	0.566167	-1662.2569553	-1661.792196	-1662.661228	-1662.196468
Me-D1_{tBu}	0.568480	-1662.2855028	-1661.818947	-1662.688576	-1662.222021
Me-TSD1-D3_{tBu}	0.566120	-1662.2421216	-1661.778527	-1662.647687	-1662.184093
Me-D3_{tBu}	0.570452	-1662.3080075	-1661.837151	-1662.713185	-1662.242329
Me-TSD3-F1_{tBu}	0.567077	-1662.2516856	-1661.785438	-1662.657155	-1662.190908
Me-F1_{tBu}	0.569788	-1662.2766791	-1661.806154	-1662.682184	-1662.211659
Me-TSF1-F2_{tBu}	0.568324	-1662.2674063	-1661.796648	-1662.675037	-1662.204278
Me-F2_{tBu}	0.568444	-1662.2750812	-1661.805625	-1662.68385	-1662.214394
Me-TSF2-F3_{tBu}	0.564089	-1662.2576718	-1661.794852	-1662.666855	-1662.204035
Me-F3_{tBu}	0.565627	-1662.2598337	-1661.794837	-1662.669815	-1662.204818
Me-TSF3-F4_{tBu}	0.565716	-1662.2493854	-1661.783789	-1662.657663	-1662.192066
Me-F4_{tBu}	0.565421	-1662.2691757	-1661.804158	-1662.676616	-1662.211598
Me-TSF4-product 3_{tBu}	0.565518	-1662.2597468	-1661.793555	-1662.667416	-1662.201225
Me-product3_{tBu}	0.550621	-1311.2345701	-1310.771393	-1311.572586	-1311.109409
Me-G1_{tBu}	0.568461	-1662.299796	-1661.833956	-1662.707596	-1662.241756
Me-TSG1-product 4_{tBu}	0.564540	-1662.2642034	-1661.804675	-1662.67011	-1662.210582
Me-product 4_{tBu}	0.550248	-1311.2564785	-1310.791949	-1311.593389	-1311.12886
Me-C2_{Me}	0.483002	-1544.439474	-1544.052825	-1544.819055	-1544.432406
Me-TSC2-C3_{Me}	0.482349	-1544.439094	-1544.052256	-1544.818624	-1544.431786

Me-C3_{Me}	0.483232	-1544.444956	-1544.058376	-1544.82355	-1544.43697
Me-TSC3-C4_{Me}	0.484650	-1544.433597	-1544.04242	-1544.816524	-1544.425347
Me-C4_{Me}	0.483636	-1544.441628	-1544.055191	-1544.823062	-1544.436625
Me-TSC4-C5_{Me}	0.482908	-1544.426096	-1544.039197	-1544.805132	-1544.418233
Me-C5_{Me}	0.483690	-1544.430591	-1544.042736	-1544.80778	-1544.419925
Me-TSC5-C6_{Me}	0.481543	-1544.422978	-1544.039844	-1544.80742	-1544.424285
Me-C6_{Me}	0.481795	-1544.425222	-1544.042339	-1544.808364	-1544.425481
Me-TSC6-C7_{Me}	0.480215	-1544.424887	-1544.042417	-1544.807854	-1544.425384
Me-C7_{Me}	0.481850	-1544.431492	-1544.048563	-1544.814667	-1544.431738
Me-TSC7-C8_{Me}	0.482198	-1544.417659	-1544.03256	-1544.801386	-1544.416287
Me-C8_{Me}	0.482927	-1544.425484	-1544.042872	-1544.809469	-1544.426857
Me-TSC8-C9_{Me}	0.482491	-1544.423984	-1544.039118	-1544.80706	-1544.422194
Me-C9_{Me}	0.483644	-1544.439252	-1544.052939	-1544.82266	-1544.436347
Me-TSC9-G1_{Me}	0.482605	-1544.431706	-1544.045702	-1544.8152	-1544.429196

Table S2 Results of BMK single-point energy for all the species shown in Fig. 1 on the basis of the M06-optimized structures.*

Structures	M06	BMK
	Rel energy (kcal mol ⁻¹)	Rel energy (kcal mol ⁻¹)
A1_H	0.0	0.0
A2_H	9.9	3.7
TSA2-B1_H	22.4	10.3
B1_H	-8.2	-20.1
TSB1-B2_H	-8.1	-20.0
B2_H	-21.8	-34.0
TSB2-B3_H	-5.6	-20.7
B3_H	-20.3	-34.0
TSB3-B4_H	-3.8	-20.1
B4_H	-25.2	-42.5
TSB4-C1_H	-6.5	-24.3
C1_H	-22.0	-37.9

*. BMK (Boese-Martin for Kinetics) is a hybrid meta-GGA functional.